Monthly Notices
of the
ROYAL ASTRONOMICAL SOCIETY

MNRAS **466,** L48–L52 (2017)
Advance Access publication 2016 October 26

doi:10.1093/mnrasl/slw218

# Discovery of a 0.42-s pulsar in the ultraluminous X-ray source NGC 7793 P13

G. L. Israel,[1⋆] A. Papitto,[1] P. Esposito,[2,3] L. Stella,[1] L. Zampieri,[4] A. Belfiore,[3] G. A. Rodríguez Castillo,[1] A. De Luca,[3] A. Tiengo,[3,5,6] F. Haberl,[7] J. Greiner,[7] R. Salvaterra,[3] S. Sandrelli[8] and G. Lisini[5]

[1]*INAF–Osservatorio Astronomico di Roma, via Frascati 33, I-00040 Monteporzio Catone, Italy*
[2]*Anton Pannekoek Institute for Astronomy, University of Amsterdam, Postbus 94249, NL-1090-GE Amsterdam, the Netherlands*
[3]*INAF–Istituto di Astrofisica Spaziale e Fisica Cosmica - Milano, via E. Bassini 15, I-20133 Milano, Italy*
[4]*INAF–Osservatorio Astronomico di Padova, INAF, vicolo dell'Osservatorio 5, I-35122 Padova, Italy*
[5]*Scuola Universitaria Superiore IUSS Pavia, piazza della Vittoria 15, I-27100 Pavia, Italy*
[6]*INFN–Istituto Nazionale di Fisica Nucleare, Sezione di Pavia, via A. Bassi 6, I-27100 Pavia, Italy*
[7]*Max-Planck-Institut für extraterrestrische Physik, Giessenbachstraße, D-85748 Garching, Germany*
[8]*INAF–Osservatorio Astronomico di Brera, via Brera 28, I-20121 Milano, Italy*

Accepted 2016 October 18. Received 2016 October 16; in original form 2016 September 20

## ABSTRACT

NGC 7793 P13 is a variable (luminosity range ∼100) ultraluminous X-ray source proposed to host a stellar-mass black hole of less than 15 $M_\odot$ in a binary system with orbital period of 64 d and a 18–23 $M_\odot$ B9Ia companion. Within the EXTraS (Exploring the X-ray Transient and variable Sky) project, we discovered pulsations at a period of ∼0.42 s in two *XMM–Newton* observations of NGC 7793 P13, during which the source was detected at $L_X \sim 2.1 \times 10^{39}$ and $5 \times 10^{39}$ erg s$^{-1}$ (0.3–10 keV band). These findings unambiguously demonstrate that the compact object in NGC 7793 P13 is a neutron star accreting at super-Eddington rates. While standard accretion models face difficulties accounting for the pulsar X-ray luminosity, the presence of a multipolar magnetic field with $B \sim$ few $\times 10^{13}$ G close to the base of the accretion column appears to be in agreement with the properties of the system.

**Key words:** galaxies: individual: NGC 7793 – X-rays: binaries – X-rays: individual: CXOU J235750.9 – 323726 (XMMU J235751.1−323725, NGC 7793 P13).

## 1 INTRODUCTION

Ultraluminous X-ray sources (ULXs) are extranuclear point-like X-ray objects located in nearby galaxies with X-ray luminosities exceeding the Eddington limit of $>10^{39}$ erg s$^{-1}$ for a ∼10 $M_\odot$ black hole (BH). Based on their spectral and timing properties, it has been proposed (see Roberts et al. 2016 for a recent review) that most ULXs are stellar-remnant BHs (with masses possibly reaching ∼100 $M_\odot$; Zampieri & Roberts 2009; Belczynski et al. 2010) accreting at super-Eddington rates. The salient ULX features revealed by *XMM–Newton* and *NuSTAR* observations and supporting the scenario of super-Eddington accretion on to BHs is a downturn of the X-ray spectrum at energies of ∼5–10 keV and a soft excess at lower energies (Roberts et al. 2016 and references therein). Despite evidences in favour of the BH nature of the compact remnant in ULXs (Liu et al. 2013), there are also two notable exceptions of pulsating ULXs (PULXs) testifying to the presence of accreting neutron stars (NSs; Bachetti et al. 2014; Israel et al. 2016). This shows that spectral properties alone are not an unambiguous way for a correct identification of the compact remnant in ULX (Bachetti 2016).

Within the framework of the EXTraS[1] (Exploring the X-ray Transient and variable Sky; De Luca et al. 2016) project, we searched for coherent periodic signals in the about 290 000 time series of sources, with more than 50 counts, detected by *XMM–Newton* in all European Photon Imaging Camera (EPIC) public data. Among dozens of new X-ray pulsators found so far with periodic signals detected at high confidence ($>4.5\sigma$), there is XMMU J235751.1−323725 = CXOU J235750.9−323726, also known as the ULX P13 in NGC 7793.

NGC 7793 P13 was first observed in 1979 by the *Einstein* satellite as a bright, $L_X \sim 2 \times 10^{39}$ erg s$^{-1}$ (in the 0.3–10 keV range), X-ray stellar-like object in the nearby ($D = 3.9$ Mpc; Karachentsev et al. 2003; this distance is adopted throughout the Letter)

⋆ E-mail: Gianluca@mporzio.astro.it

[1] See http://www.extras-fp7.eu/.

**Table 1.** Logbook of the *XMM–Newton* observations used in this work.

| Obs. ID | Start date | Exp. (ks) | Off-axis[a] (arcsec) | Count rate[b] (cts $s^{-1}$) |
|---|---|---|---|---|
| 0693760101 | 2012-05-14 | 35 | 77 | $0.007 \pm 0.002$ |
| 0693760401 | 2013-11-25 | 45 | 77 | $0.29 \pm 0.02$ |
| 0748390901 | 2014-12-10 | 47 | 249 | $0.53 \pm 0.02$ |

*Notes*. [a]Radial off-axis angle of NGC 7793 P13 from the boresight of the telescope.
[b]Net source count rate from pn in the 0.3–10 keV energy band, using the extraction regions described in the text.

reasonably face-on ($i = 53.^{\circ}7$) galaxy NGC 7793 in the Sculptor group (Fabbiano, Kim & Trinchieri 1992). It was also detected by *ROSAT* in 1992 at $L_X \sim 3.5 \times 10^{39}$ erg $s^{-1}$ (value extrapolated in the 0.3–10 keV band; Read & Pietsch 1999). A *Chandra* pointing carried out in 2003 September revealed two sources at the *ROSAT* position of NGC 7793 P13, separated by 2 arcsec, namely CXOU J235750.9−323726 and CXOU J235750.9−323728 (Pannuti et al. 2011). The latter source is thought to be unrelated to NGC 7793 P13 and is more than an order of magnitude less luminous than NGC 7793 P13 itself. Their luminosities are $\sim 1.2 \times 10^{39}$ and $\sim 6.2 \times 10^{37}$ erg $s^{-1}$, respectively. The compact object in NGC 7793 P13 is orbiting around a B9Ia spectral-type star of 18–23 $M_{\odot}$ in a binary system with an orbital period of about 64 d and a moderate eccentricity $e$ of 0.3–0.4 (Motch et al. 2014). By modelling the strong optical and UV orbital modulation, likely arising from the heating of the donor star, a mass for the suspected BH of less than about 15 $M_{\odot}$ has been inferred for NGC 7793 P13 (Motch et al. 2014).

Here, we report on the discovery of coherent pulsations at a period of 0.42 s in the EPIC pn light curves of XMMU J235751.1−323725, with a secular first-period derivative of $\dot{P}_{\rm sec} \sim -4 \times 10^{-11}$ s $s^{-1}$ (Section 2.3). These findings clearly indicate that NGC 7793 P13 hosts an accreting NS in a binary system and not a stellar-mass BH as previously assumed. We discuss the nature of this new ultraluminous X-ray pulsar (Section 3), the third discovered so far, and also the fastest spinning one.

## 2 OBSERVATIONS AND DATA ANALYSIS

### 2.1 *XMM–Newton* and *Chandra*

The region of NGC 7793 P13 was observed by *XMM–Newton* with the EPIC detectors in full imaging mode (Full Frame). The source position was always off-axis, at angles from ∼1.2 to 4.1 arcmin. The 0.42-s pulsations were detected in the pn data only (MOS cameras time resolution ∼2.6 s; pn time resolution ∼73 ms). The public pn data sets covering the position of NGC 7793 P13 are listed in Table 1. During the first pointing, a faint source was detected at a flux level of $\sim 1.7(3) \times 10^{-14}$ erg $cm^{-2}$ $s^{-1}$, corresponding to a luminosity of $\sim 3 \times 10^{37}$ erg $s^{-1}$ and providing only about 120 events.

As part of the EXTraS reduction pipeline, the raw observation data files were processed with the Science Analysis Software (SAS) v.16. Time intervals with high particle background were filtered. Photon event lists and spectra were extracted in a radius of 32 arcsec for the source, while to estimate the background we used a nearby region with radius of 45 arcsec, far from other sources and avoiding CCD gaps. Event times were converted to the barycentre of the Solar system with the SAS task BARYCEN using the *Chandra* source position (RA = $23^{\rm h}57^{\rm m}50.^{\rm s}9$, Dec. = $-32^{\circ}37'26.''6$). Spectra were rebinned so as to obtain a minimum of 30 counts per energy bin,

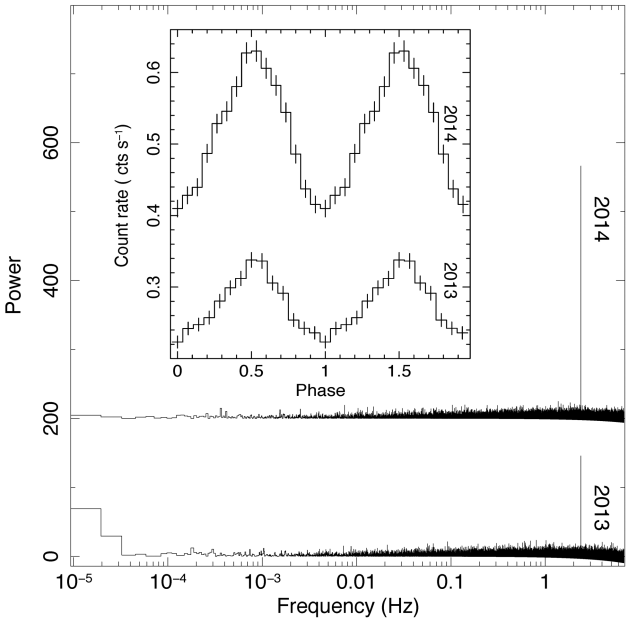


**Figure 1.** Fourier power spectra for the 2013 November (bottom) and 2014 December (top; shifted by +200 in power) pn data (0.1–12 keV; $\Delta t \simeq 73$ ms, 524 288 frequencies). The prominent peaks at about 2.4 Hz correspond to the 0.42-s signal. The inset shows the background subtracted light curves of the two data sets folded to their best periods (see Table 2.)

and for each spectrum we generated the response matrix and the ancillary file using the SAS tasks RMFGEN and ARFGEN.

NGC 7793 P13 was imaged four times by *Chandra* between 2003 (one pointing) and 2011 (three pointings) with the Advanced CCD Imaging Spectrometer (time resolution of 3.2 s) at an off-axis angle between 2 and 4.5 arcsec. We used WAVDETECT (within the CIAO package, v.4.8) for source detection and considered six wavelet detection scales (1, 2, 4, 8, 12 and 16 pixels). Spectra were obtained in the 0.3–10 keV energy range using the SPECEXTRACT, circular regions of 4 arcsec for the source, and locally optimized background regions for each observation. As a result of this analysis, we detect only one source at the position of NGC 7793 P13 in all observations (at variance with Pannuti et al. 2011). In the following, we assume that the faint source detected by *Chandra* (2011) and *XMM–Newton* (2012) is indeed NGC 7793 P13.

### 2.2 *Swift*

We analysed the 78 observations of NGC 7793 performed with the *Swift* X-Ray Telescope (Burrows et al. 2005) between 2010 August 16 and 2016 August 24, for a total exposure of 210 ks. We processed and analysed the observations performed in photon counting mode using the standard software (HEASOFT v. 6.19) and calibration files (CALDB v. 20160609). We extracted source photons in a 20-pixel radius (equivalent to 47.2 arcsec) around the source position; background was extracted from close-by source-free regions. Photons with grade between 0 and 12 were retained in the analysis.

### 2.3 Discovery of the period and timing analysis

A periodic signal at about 0.42 s was first detected in the 0.1–12 keV pn data set 0748390901 (2014 December) at a confidence level (c.l.) of about $13\sigma$ by the power spectrum peak detection algorithm of the automatic analysis (Israel & Stella 1996; see Fig. 1 and Table 2).

**Table 2.** Main properties of the NGC 7793 P13 pulsar.

| Epoch (MJD TDB) | 56621.0 | 57001.0 |
|---|---|---|
| $P$ (s) | 0.419 7119(2) | 0.418 3891(1) |
| $\nu$ (Hz) | 2.382 586(1) | 2.390 1207(6) |
| $\lvert\dot{P}\rvert$ ($10^{-11}$ s s$^{-1}$) | <10 | <5 |
| $\dot{P}_{\rm sec}$ ($10^{-11}$ s s$^{-1}$) | −4.031(4) | |
| Pulsed fraction ( per cent)[a] | 18(1) | 22(1) |
| $F_{\rm X}^{0.3-10}$ (erg cm$^{-2}$ s$^{-1}$) | $1.1(1)\times10^{-12}$ | $2.7(1)\times10^{-12}$ |
| $L_{\rm X}^{0.3-10}$ (erg s$^{-1}$) | $2.1(2)\times10^{39}$ | $5.0(2)\times10^{39}$ |

*Note*. [a]Pulsed fraction defined as the semi-amplitude of the sinusoid divided by the average source count rate in the 0.1–12 keV range.

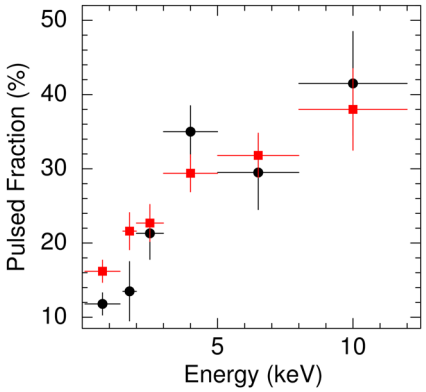


**Figure 2.** Background subtracted pulsed fractions of the 0.42-s signal as a function of energy for the 2013 (circles) and 2014 (squares) pn data.

By a phase fitting analysis, we honed the period at 0.4183891 ± 0.0000001 s (with uncertainty at 1$\sigma$ c.l.). No significant first-period derivative was found, with 3$\sigma$ limits of about $\pm5\times10^{-11}$ s s$^{-1}$. Pulsations at about 0.42 s were also detected in the pn data of Obs. 069376040, carried out one year before (2013 November). The refined period value was 0.4197119 ± 0.0000002 s. Also in this data set, no first-period derivative was found (with 3$\sigma$ limits of about $\pm10^{-10}$ s s$^{-1}$), but the difference between the two measures implies a long-term average (secular) period derivative $\dot{P}_{\rm sec}=-(4.031\pm0.004)\times10^{-11}$ s s$^{-1}$.

The 0.1–12 keV pulse profiles are almost sinusoidal (single-peaked), with an averaged pulsed fraction of 18 ± 1 per cent and 22 ± 1 per cent for the 2013 and 2014 observations, respectively (see inset in Fig. 1). The pulsed fraction is increasing from 10 to 20 per cent below 1.5 keV up to about 40 per cent above 8 keV (see Fig. 2).

### 2.4 Spectral analysis and long-term variability

The spectral fitting was performed in 0.3–10 keV using XSPEC v.12.8; the abundances used are those of Wilms, Allen & McCray (2000). Different spectral models have been used in literature to fit the 2013 *XMM–Newton* spectrum of NGC 7793 P13 (Motch et al. 2014). Bearing in mind the nature of the compact object, we simply notice that a good fit can be also obtained assuming an empirical model often used for accreting X-ray pulsars in our Galaxy: an absorbed power-law with a high-energy cut-off (the multiplicative component HIGHECUT in XSPEC) plus, sometimes, a soft thermal component at low energies, which we modelled with a blackbody (BB). A similar model has been successfully tested on the X-ray spectra of a sample of ULXs with broad-band *XMM+NuSTAR* data by Pintore et al. (2016). We note that, regardless of the model used, the fluxes and luminosities derived do not change significantly. The model PHABS[HIGHECUT*(POWERLAW+BBODYRAD)] gave the following parameters (we assumed that the two data sets have the same absorption): $N_{\rm H}=(9.60\pm0.01)\times10^{20}$ cm$^{-2}$, $\Gamma^{2013}=1.2\pm0.1$ and $\Gamma^{2014}=1.14\pm0.06$, $E_{\rm cut}^{2013}=5.5^{+0.8}_{-0.5}$ keV and $E_{\rm cut}^{2014}=6.5^{+0.4}_{-0.6}$ keV, $E_{\rm fold}^{2013}=5.0\pm1.7$ keV and $E_{\rm fold}^{2014}=4.6^{+1.5}_{-0.9}$ keV, $kT_{\rm BB}^{2013}=0.18\pm0.02$ keV and $kT_{\rm BB}^{2014}=0.23\pm0.04$ keV, $R_{\rm BB}^{2013}=(1.2\pm0.3)\times10^3$ km and $R_{\rm BB}^{2014}=(0.7\pm0.1)\times10^3$ km (90 per cent c.l. uncertainties are reported; see also Table 2 for fluxes and luminosities; see Fig. 3). We note that the size of the BB is of the order of the corotation radius of the pulsar (see below). The probabilities, as inferred through the Fisher test, that the inclusion of the HIGHECUT component (with respect to the power law alone) and of the BB component (with respect to HIGHECUT*POWERLAW) are not needed are $7\times10^{-17}$ and $9\times10^{-12}$, respectively. The reduced $\chi^2$ for the simultaneous fit of the two data sets is 1.13 for 373 degrees of freedom (dof). For the 2011 *Chandra* spectra, we considered a simple absorbed power-law model due to poor statistics, and compared the results with those of the brightest *Chandra* (2003) and *XMM–Newton* (2014) observations (adopting the same model and keeping the same value for $N_{\rm H}$). We obtained the following value for the photon index: $\Gamma^{2011}=1.5(2)$, $\Gamma^{2003}=1.21(3)$ and $\Gamma^{2014}=1.29(2)$ at 90 per cent c.l., suggesting a moderate steepening of the spectrum at lower fluxes.

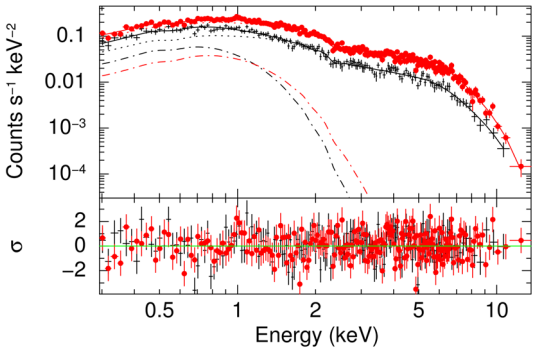


**Figure 3.** *XMM–Newton* pn energy spectra of NGC 7793 P13 fitted with the blackbody (dot–dashed line) plus power-law (dotted line) model described in Section 2.4 for the 2013 (crosses) and 2014 (filled circles). The residuals, in unit of $\sigma$, are also plotted (lower panel).

The data from the *Swift* monitoring proved useful to study the long-term variability of NGC 7793 P13. We fit simultaneously the spectra in the 0.3–10 keV band, using the Cash (C) statistics and after binning energy channels so as to have at least one count per bin. We assumed an absorbed power-law model, forcing the absorption column to take the same (free) value in all the observations. The C statistics we obtained was 3906 for 4595 dof. We measured an absorption column density of $N_{\rm H}=(6.7\pm0.2)\times10^{20}$ cm$^{-2}$. The average value of the index of the power law was $\langle\Gamma\rangle=1.03$, with a standard deviation of 0.18. The observed 0.3–10 keV unabsorbed fluxes are plotted in Fig. 4; the right scale of the plot represents the isotropic luminosity in the same energy band. When the source was not significantly detected, we set an upper limit on the 0.3–10 keV count rate at 3$\sigma$ c.l. following Gehrels (1986). Then, we converted the count rate into a flux estimate with WebPIMMS,[2] assuming that the spectrum is described by an absorbed power law with absorption

[2] See https://heasarc.gsfc.nasa.gov/cgi-bin/Tools/w3pimms/w3pimms.pl.

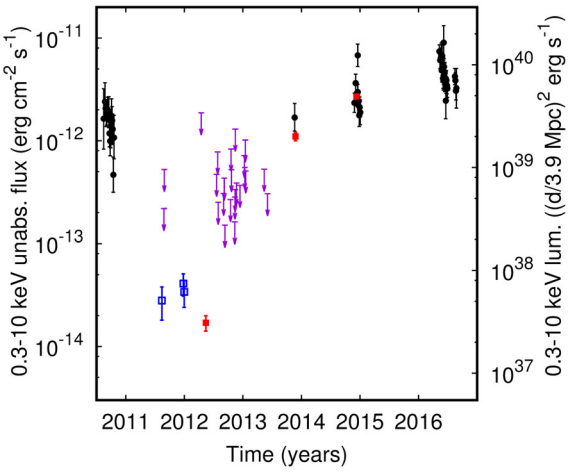


**Figure 4.** Long-term 0.3–10 keV flux (left axis) and isotropic luminosity (right axis) evolution of NGC 7793 P13 as observed by *Swift* (filled circles), *XMM–Newton* (filled squares) and *Chandra* (empty squares). Arrows mark the $3\sigma$ upper limits derived from individual *Swift* (purple) observations.

column $N_{\rm H} = 5.7 \times 10^{20}$ cm$^{-2}$ and photon index $\Gamma = 1$ (see arrows in Fig. 4).

NGC 7793 P13 was detected in X-ray outburst during observations performed in 2010, and from late 2013 to 2016. The maximum and minimum observed 0.3–10 keV flux are $9^{+4}_{-3} \times 10^{-12}$ and $(0.5 \pm 0.2) \times 10^{-12}$ erg cm$^{-2}$ s$^{-1}$ observed on 2016 June 6 and 2010 October 15, respectively. These fluxes translate into 0.3–10 keV isotropic luminosity of $\sim$1.6 $\times$ $10^{40}$ and $\sim$9 $\times$ $10^{38}$ erg s$^{-1}$. A bolometric correction factor of $\sim$1.25 is obtained if it is assumed that the spectrum is cut off at $E_{\rm cut} = 5.5$ keV with a folding energy of $E_{\rm fold} = 5$ keV.

## 3 DISCUSSION

Motch et al. (2014) found that the orbital period of NGC 7793 P13 is 64 d, and that the properties of the optical counterpart are consistent with those of a B9Ia supergiant companion with mass in the range $M_2 = 18$–$23\,{\rm M}_\odot$ and radius of $R_2 = 50$–$60\,{\rm R}_\odot$. The same authors assume that the star fills its Roche lobe, since the stellar wind from a B9Ia supergiant cannot provide the accretion rate needed to produce the maximum observed X-ray luminosity ($10^{19}$–$10^{20}$ g s$^{-1}$, see below). All acceptable orbital solutions require a significant eccentricity ($e = 0.27$–$0.41$). From this constraint, Motch et al. (2014) conclude that, at periastron, the supergiant can fill its Roche lobe for a BH companion with a mass $3.4\,{\rm M}_\odot < M_{\rm BH} < 15\,{\rm M}_\odot$, with the upper limit being fixed by the requirement that the Roche lobe is not too small to accommodate the star.

The discovery of a pulsar in NGC 7793 P13 allows us to place an independent and even tighter constraint on the orbital eccentricity of the system. Assuming a mass $M_1 = 1.4\,{\rm M}_\odot$ for the NS, the Roche lobe of the companion is bigger than that for a BH. Therefore, for a 64 days orbital period, even a B9Ia supergiant cannot fill it unless the eccentricity is $e = 0.46$–$0.55$, so that, at periastron, the separation is sufficiently small to allow for a contact phase.

Following Motch et al. (2014), we assume that the mass transfer in the system proceeds on a thermal time-scale $t_{\rm th}$: $t_{\rm th} = 2.4 \times 10^5 (M_2/20\,{\rm M}_\odot)^2 \times (R_2/50\ {\rm R}_\odot)^{-1} (L_2/10^4\,{\rm L}_\odot)^{-1}\,{\rm yr}$, where $L_2$ is the luminosity of the companion. The mass transfer rate is then as follows: $\dot{M}_2 \approx M_2/t_{\rm th} = 3.7 \times 10^{21} (M_2/20\,{\rm M}_\odot)^{-1} \times (R_2/50\,{\rm R}_\odot)(L_2/10^4\,{\rm L}_\odot)\,{\rm g\,s^{-1}}$. Owing to the large mass ratio ($q = M_2/M_1 \gg 1$), the evolution is expected to be non-conservative. Part of the mass is likely to be removed from the binary through hydrodynamical instabilities, although the system may possibly be stabilized by the significant mass-loss of the companion (Fragos et al. 2015). Even considering all mass-losses, $\dot{M}_2$ is so high to easily account for the accretion rate $\dot{M}$ implied by the maximum observed X-ray luminosity: $L_{\rm max} \approx b \times 10^{40}\,{\rm erg\,s^{-1}}$, $\dot{M} = L_{\rm max}/(\eta c^2) \approx 10^{20} b\,(0.1/\eta)\,{\rm g\,s^{-1}}$, where $b$ is the beaming factor and $\eta$ the accretion efficiency (see also below).

NGC 7793 P13 displayed a factor of $\sim$8 flux variation in the high state (above $\sim 2 \times 10^{39}$erg s$^{-1}$; see Fig. 4), attaining a maximum isotropic luminosity of $L_{\rm iso}^{\rm max} \sim 1.6 \times 10^{40}$ erg s$^{-1}$, about 100 times higher than the Eddington limit. We note that the $\sim$0.42-s pulsations were observed at the top and close to the bottom of this range, implying that accretion on to the NS took place over the entire interval of variation.

In our discussion here, we assume that accretion on to the NS takes place unimpeded (at least) over the above-mentioned luminosity variation. The $\sim -4.0 \times 10^{-11}$ s s$^{-1}$ period derivative, inferred from the two one-year-apart observations during which pulsations were detected, is virtually unaffected by orbital Doppler shift given that the two *XMM–Newton* pointings are almost at the same orbital phase (assuming $P_{\rm orb} = 63.52$ d; Motch et al. 2014).

NSs may attain accretion luminosities exceeding the Eddington limit by orders of magnitude if their surface magnetic field ($B$) is very high, so that electron scattering cross-sections for extraordinary mode photons below the cyclotron energy $E_{\rm c} \sim 12 (B/10^{12}\,{\rm G})$ keV is much lower than the Thomson cross-section. Mushtukov et al. (2015) show that column accretion on to a $>10^{15}$ G magnetic pole may give rise to a luminosity of $L \sim 10^{41}$ erg s$^{-1}$. However, for a magnetic NS to accrete at a very high rate, other conditions must be met. First, the accretion flow outside the magnetosphere must take place through a disc which remains geometrically thin (i.e. height/radius ratio $<1$), such that the bulk of the flux emitted close to the bottom of the accretion column can escape. This translates into the condition that the accretion energy released in the disc down to the magnetospheric radius $r_{\rm m}$ is sub-Eddington (dashed line in Fig. 5). An additional condition is that the NS angular velocity is smaller than the (Keplerian) angular velocity of the disc at $r_{\rm m}$, so that the drag exerted by the rotating magnetic field lines as matter enters the magnetosphere is weaker than gravity, and matter can accrete on to the surface. This is equivalent to requiring that $r_{\rm m} < r_{\rm cor}$, where $r_{\rm cor} = \left(\frac{GMP^2}{4\pi^2}\right)^{1/3}$ is the corotation radius (Illarionov & Sunyaev 1975; Stella, White & Rosner 1986). When $r_{\rm m} > r_{\rm cor}$, centrifugal forces at $r_{\rm m}$ exceed gravity and only little accretion, if any, can take place when the so-called propeller regime ensues (dot–dashed line in Fig. 5). For NGC 7793 P13 to emit isotropically a maximum luminosity of $L_{\rm iso}^{\rm max} \sim 1.6 \times 10^{40}$ erg s$^{-1}$ according to the model of Mushtukov et al. (2015), the NS surface dipolar magnetic should be at least $B \sim 2 \times 10^{14}$ G. However, for such value of $B$ and $P \sim 0.42$ s, accretion would be inhibited by magnetospheric drag, and the NS would be deep in the propeller regime.

Therefore, we relax the assumption of isotropy, and consider that the NS emission is beamed by a factor $b < 1$. In this case, the isotropic equivalent luminosity is $L_{\rm iso} = L_{\rm acc}/b$, and the accretion luminosity $L_{\rm acc} = GM\dot{M}/R$ is reduced correspondingly (here, $R$ and $M$ are the NS radius and mass). We assume that the minimum (detected) isotropic luminosity of $L_{\rm iso}^{\rm min} \sim L_{\rm iso}^{\rm max}/8$ marks the onset of the transition from accretion to the propeller phase (i.e. $r_{\rm m} = r_{\rm cor}$) and, at the same time, require that the surface magnetic field is high enough to attain the observed luminosity range (solid line in Fig. 5).

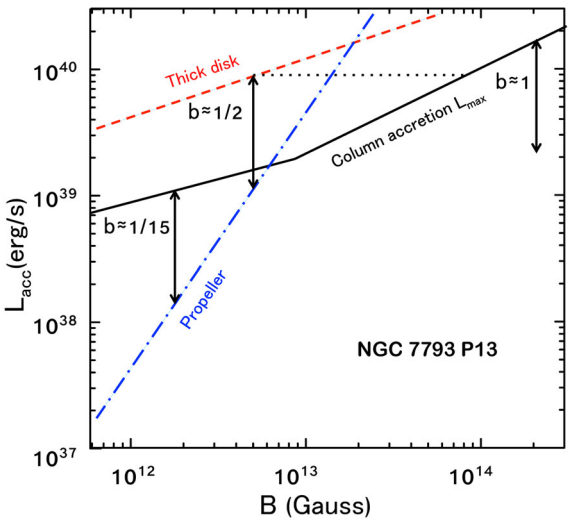


**Figure 5.** Accretion luminosity versus surface magnetic field constraints for NGC 7793 P13. The solid line gives the maximum luminosity which can be produced by column accretion on to the NS magnetic poles. The dashed line is the limit above which the energy released in the accretion disc exceeds the Eddington limit and disc thickens. Accretion is inhibited below the dot–dashed line, as the NS enters the propeller regime. Double-arrowed segments show the factor of ∼8 flux variation displayed by the source when pulsations were detected. Different segments are shifted by the inverse of the beaming factor $b^{-1} = L_{\rm iso}/L_{\rm acc}$. A value of $b \sim 1/2$ is found to be in agreement with the observed source properties (see the text): this solution implies a dipole magnetic field of $B \sim 5 \times 10^{12}$ G and a multipolar field $B > 8 \times 10^{13}$ G at the base of the accretion column (dotted line).

A surface dipole field of $B \sim 2 \times 10^{12}$ G and a maximum accretion luminosity of $L_{\rm acc} \sim 10^{39}$ erg s$^{-1}$ are obtained, corresponding to beaming factor of $b \sim 1/15$ (note that for these parameters the disc remains geometrically thin). For a time-averaged accretion rate of $\dot{M} \sim 3 \times 10^{18}$ g s$^{-1}$, as implied by this solution, we estimate the corresponding maximum spin-up rate by imposing that the matter accreting on to the NS carries the Keplerian angular momentum at $r_{\rm cor}$. This gives a maximum $\dot{P} = \dot{M}\, r_{\rm cor}^2 P/I \sim -1 \times 10^{-11}$ s s$^{-1}$, four times smaller than the secular $\dot{P}$ derived from the data.

In order to ease this problem, and by analogy with the case of NGC 5907 ULX-1 (Israel et al. 2016), we consider the possibility that close to the NS surface (and thus the base of the accretion column) the magnetic field is dominated by higher than dipole magnetic multipoles. Close to the magnetospheric radius ($r_{\rm m} \sim 10^8$ cm), the field is virtually the dipolar by virtue of its less steep radial dependence. This is done by analogy with the case of magnetars (Thompson & Duncan 1995; Tiengo et al. 2013). The conditions that the accretion disc is thin for $L_{\rm iso}^{\rm max} = L_{\rm acc}^{\rm max}/b$ and that the NS is in the accretion regime for $L_{\rm iso}^{\rm min} = L_{\rm acc}^{\rm min}/b$ depend on the B-field strength at $r_{\rm m}$, where only the dipole component matters. Both conditions are satisfied for $B$ of $\sim 5 \times 10^{12}$ G and $b \sim 1/2$. A (multipolar) $B > 8 \times 10^{13}$ G at the base of the accretion column would be required to give rise to corresponding maximum accretion luminosity of $L_{\rm acc}^{\rm max} = 9 \times 10^{39}$ erg s$^{-1}$(dotted line in Fig. 5). A maximum spin-up of $\dot{P} \sim -7 \times 10^{-11}$ s s$^{-1}$ is derived in this case (owing to the higher time-averaged accretion rate resulting from $b \sim 1/2$), consistent with the value inferred from the observations. For a ∼0.42-s spin period, we expect that the isotropic luminosity in the propeller regime is $< L_{\rm iso}^{\rm min}/90 \sim 2 \times 10^{37}$ erg s$^{-1}$(Corbet et al. 1997), a level which is slightly below the values inferred during the 2011 *Chandra* and 2012 *XMM–Newton* observations, to within uncertainties.

The discovery of three PULXs previously classified as stellar mass BH based on their spectral properties strongly suggests that this class might be more numerous than suspected so far, and that other know ULXs might host an accreting NS. The large first-period derivative, the intermittence of the pulsations and their relatively small pulsed fraction make their detection a difficult task.

## ACKNOWLEDGEMENTS

EXTraS is funded from the EU's Seventh Framework Programme under grant agreement no. 607452. PE acknowledges funding in the framework of the NWO Vidi award A.2320.0076. LZ and GLI acknowledge funding from the ASI - INAF contract NuSTAR I/037/12/0. AP acknowledges support via an EU Marie Sklodowska-Curie Individual Fellowship under contract No. 660657-TMSP-H2020-MSCA-IF-2014. After submission, we became aware of the manuscript by Füerst et al. (2016) which confirmed the discovery.

## REFERENCES

Bachetti M., 2016, Astron. Nachr., 337, 349
Bachetti M. et al., 2014, Nature, 514, 202
Belczynski K., Bulik T., Fryer C. L., Ruiter A., Valsecchi F., Vink J. S., Hurley J. R., 2010, ApJ, 714, 1217
Burrows D. N. et al., 2005, Space Sci. Rev., 120, 165
Corbet R. H. D., Charles P. A., Southwell K. A., Smale A. P., 1997, ApJ, 476, 833
De Luca A., Salvaterra R., Tiengo A., D'Agostino D., Watson M. G., Haberl F., Wilms J., 2016, in Caraveo P., D'Avanzo P., Gehrels N., Tagliaferri G., eds, Proc. Sci., Vol. 233, Swift: 10 Years of Discovery. Springer International Publishing, Switzerland, p. 135
Fabbiano G., Kim D.-W., Trinchieri G., 1992, ApJS, 80, 531
Fragos T., Linden T., Kalogera V., Sklias P., 2015, ApJ, 802, L5
Füerst F. et al., 2016, ApJ, in press
Gehrels N., 1986, ApJ, 303, 336
Illarionov A. F., Sunyaev R. A., 1975, A&A, 39, 185
Israel G. L., Stella L., 1996, ApJ, 468, 369
Israel G. et al., 2016, preprint (arXiv:1609.07375)
Karachentsev I. D. et al., 2003, A&A, 404, 93
Liu J.-F., Bregman J. N., Bai Y., Justham S., Crowther P., 2013, Nature, 503, 500
Motch C., Pakull M. W., Soria R., Grisé F., Pietrzyński G., 2014, Nature, 514, 198
Mushtukov A. A., Suleimanov V. F., Tsygankov S. S., Poutanen J., 2015, MNRAS, 454, 2539
Pannuti T. G., Schlegel E. M., Filipović M. D., Payne J. L., Petre R., Harrus I. M., Staggs W. D., Lacey C. K., 2011, AJ, 142, 20
Pintore F., Zampieri L., Stella L., Walter A., Mereghetti S., Israel G. L., 2016, MNRAS, in press
Read A. M., Pietsch W., 1999, A&A, 341, 8
Roberts T. P., Middleton M. J., Sutton A. D., Mezcua M., Walton D. J., Heil L. M., 2016, Astron. Nachr., 337, 534
Stella L., White N. E., Rosner R., 1986, AJ, 308, 669
Thompson C., Duncan R. C., 1995, MNRAS, 275, 255
Tiengo A. et al., 2013, Nature, 500, 312
Wilms J., Allen A., McCray R., 2000, ApJ, 542, 914
Zampieri L., Roberts T. P., 2009, MNRAS, 400, 677

This paper has been typeset from a TEX/LATEX file prepared by the author.